Influence of Sodium-Calcium Exchange on Calcium Current Rundown and the Duration of Calcium-dependent Chloride Currents in Pituitary Cells, Studied with Whole Cell and Perforated Patch Recording

STEPHEN J. KORN and RICHARD HORN

From the Neurosciences Department, Roche Institute of Molecular Biology, Nutley, New Jersey 07110

ABSTRACT The whole cell patch-clamp technique, in both standard and perforated patch configurations, was used to study the influence of Na^+-Ca^{++} exchange on rundown of voltage-gated Ca^{++} currents and on the duration of tail currents mediated by Ca^{++}-dependent Cl^- channels. Ca^{++} currents were studied in GH_3 pituitary cells; Ca^{++}-dependent Cl^- currents were studied in AtT-20 pituitary cells. Na^+-Ca^{++} exchange was inhibited by substitution of tetraethylammonium (TEA^+) or tetramethylammonium (TMA^+) for extracellular Na^+. Control experiments demonstrated that substitution of TEA^+ for Na^+ did not produce its effects via a direct interaction with Ca^{++}-dependent Cl^- channels or via blockade of Na^+-H^+ exchange. When studied with standard whole cell methods, Ca^{++} and Ca^{++}-dependent Cl^- currents ran down within 5–20 min. Rundown was accelerated by inhibition of Na^+-Ca^{++} exchange. In contrast, the amplitude of both Ca^{++} and Ca^{++}-dependent Cl^- currents remained stable for 30–150 min when the perforated patch method was used. Inhibition of Na^+-Ca^{++} exchange within the first 30 min of perforated patch recording did not cause rundown. The rate of Ca^{++}-dependent Cl^- current deactivation also remained stable for up to 70 min in perforated patch experiments, which suggests that endogenous Ca^{++} buffering mechanisms remained stable. The duration of Ca^{++}-dependent Cl^- currents was positively correlated with the amount of Ca^{++} influx through voltage-gated Ca^{++} channels, and was prolonged by inhibition of Na^+-Ca^{++} exchange. The influence of Na^+-Ca^{++} exchange on Cl^- currents was greater for larger currents, which were produced by greater influx of Ca^{++}. Regardless of Ca^{++} influx, however, the prolongation of Cl^- tail currents that resulted from inhibition of Na^+-Ca^{++} exchange was modest. Tail currents were prolonged within tens to hundreds of milliseconds of switching from Na^+- to TEA^+-containing bath solutions. After inhibition of Na^+-Ca^{++}

Address reprint requests to Dr. Stephen J. Korn, Neuroscience Department, Roche Institute of Molecular Biology, Nutley, NJ 07110.

J. GEN. PHYSIOL. © The Rockefeller University Press · 0022-1295/89/11/0789/24 $2.00
Volume 94 November 1989 789–812

exchange, tail current decay kinetics remained complex. These data strongly suggest that in the intact cell, Na^+-Ca^{++} exchange plays a direct but nonexclusive role in limiting the duration of Ca^{++}-dependent membrane currents. In addition, these studies suggest that the perforated patch technique is a useful method for studying the regulation of functionally relevant Ca^{++} transients near the cytoplasmic surface of the plasma membrane.

INTRODUCTION

Anterior pituitary cells secrete a variety of hormones in response to a rise in intracellular calcium (Ca^{++}). With few exceptions (e.g., Luini et al., 1985), substances that stimulate secretion raise intracellular Ca^{++} levels (cf. Luini et al., 1985; Kolesnick and Gershengorn, 1986), while substances that inhibit secretion suppress rises in intracellular Ca^{++} (Luini et al., 1986; Schlegel et al., 1987). Both primary and clonal anterior pituitary cells maintain spontaneous, Ca^{++}-mediated action potentials, whose firing frequency can be modulated by secretagogues and inhibitors of secretion (Kidokoro, 1975; Taraskevich and Douglass, 1977; Suprenant, 1982; Adler et al., 1983; Schlegel et al., 1987). The extracellular space appears to be the primary source of Ca^{++} for secretagogue-induced rises in intracellular Ca^{++} and secretion (Axelrod and Reisine, 1984; Luini et al., 1985; Zatz and Reisine, 1985). Together, these data suggest that Ca^{++} entry during action potentials is an important source of Ca^{++} for secretion, and that regulation of pituitary cell electrical behavior is an important modulatory mechanism for the secretory process.

Several ion channel types, including voltage-gated Ca^{++} channels, and Ca^{++}-dependent potassium (K^+) and chloride (Cl^-) channels, underly pituitary cell excitability (Suprenant, 1982; Wong et al., 1982; Adler et al., 1983; Dubinsky and Oxford, 1984; DeRiemer and Sakmann, 1986; Korn and Weight, 1987; Mollard et al., 1987; Ritchie, 1987). The Ca^{++}-dependent channels rely on elevation of intracellular Ca^{++} for activation, and depend to a great extent on decreases in intracellular Ca^{++} for deactivation (Barrett et al., 1982; Korn and Weight, 1987). Under normal physiological conditions, three mechanisms are thought to be important for removal of excess free calcium from the cytoplasmic compartment: Na^+-Ca^{++} exchange across the plasma membrane (Blaustein et al., 1978; Gill et al., 1984; Kaczorowski et al., 1984), ATP-driven Ca^{++} sequestration and extrusion (Barros and Kaczorowski, 1984; Byerly and Yazejian, 1986), and binding of Ca^{++} to intracellular Ca^{++}-binding sites (cf. Barish and Thompson, 1983). However, the mechanisms involved in lowering the Ca^{++} concentration near the Ca^{++}-dependent channels, which could include any of these three mechanisms and/or diffusion, are not known.

The studies presented in this paper utilized two clonal anterior pituitary cell lines, GH_3 and AtT-20, to examine the functional role of Na^+-Ca^{++} exchange in the removal of intracellular Ca^{++} near Ca^{++}-sensitive channels in the plasma membrane. Specifically, two questions are addressed: (*a*) does Na^+-Ca^{++} exchange influence Ca^{++}-dependent rundown of Ca^{++} channel function? and (*b*) does Na^+-Ca^{++} exchange directly influence the time course of tail currents mediated by Ca^{++}-dependent Cl^- channels?

The standard tool for studies of this type is the whole cell patch clamp. This

method, however, suffers from two significant drawbacks. First, processes that depend on soluble intracellular biochemicals rapidly run down after the rupture of the membrane patch under the electrode. One well-known example of rundown is the loss of calcium channel function. Typically, Ca^{++} channel rundown is retarded by addition to the pipette solution of biochemicals that inhibit proteolysis and support phosphorylation (Doroshenko et al., 1982, 1984; Forscher and Oxford, 1985; Chad and Eckert, 1986; Belles et al., 1988*a*). However, prevention of rundown by this strategy can limit the ability to study channel modulation if the modulation involves endogenous counterparts to these added substances.

The second major drawback to standard whole cell recording is the disruption of endogenous cellular Ca^{++} buffering mechanisms. Although a functional plasma membrane Na^+-Ca^{++} exchange mechanism is retained in AtT-20 cells during standard whole cell recordings, its influence in cells studied with the standard technique depends on the amount of exogenous Ca^{++} buffer (i.e., EGTA) that is added to the recording solution (Korn and Weight, 1987). Energy-dependent buffering mechanisms are likely to run down due to loss of ATP or other necessary biochemicals, and diffusable Ca^{++} binding proteins probably wash out of their natural cellular compartments. Finally, additional mechanisms for Ca^{++} removal are introduced in standard whole cell recordings: that of Ca^{++} diffusion out of the cell through the ruptured membrane patch and the addition of exogenous Ca^{++} buffers.

In this paper, we used the perforated patch technique (Horn and Marty, 1988) to prevent washout of voltage-activated Ca^{++} currents and to maintain endogenous Ca^{++} buffering mechanisms during recordings of whole cell currents. Some of these results have been presented in abstract form (Horn et al., 1988; Korn and Horn, 1989).

METHODS

Cell Culture

AtT-20s (kindly provided by the Laboratory of Cell Biology, National Institutes of Health) were grown in Dulbecco's modified Eagle's medium (#320-1965; Gibco, Grand Island, NY) containing 10% fetal calf serum (FCS; Gibco); GH_3s were grown in Ham's F10 (#320-1550; Gibco) containing 2.5% FCS and 12.5% horse serum. Once a week, cells were detached from the culture flasks by a brief exposure to phosphate-buffered saline free of Ca^{++} and Mg^{++} (#17-515Y; Whittaker Bioproducts, Walkersville, MD), with 1 mM EDTA added. Cells were gently triturated and replated into Nunc 35-mM culture dishes (Laboratory Disposable Products, Haledon, NJ). AtT-20s (passage 18–35) in dishes were fed three times per week, and were used for experiments 6–8 d after replating. GH_3s (passage 27–56) were used 3–8 d after replating, and were fed 2–3 d before use.

Patch-Clamp Recording

Two voltage-clamp recording configurations were used to study macroscopic currents: the standard whole cell configuration (Hamill et al., 1981) and the newly developed, perforated patch configuration (see below and Horn and Marty, 1988). All recordings were made using the Axopatch II patch-clamp amplifier (Axon Instruments Inc., Burlingame, CA). Patch pipettes were fabricated from N51A glass (Garner Glass Co., Claremont, CA), coated with Sylgard (Dow Corning Corp., Midland, MI), and fire-polished. The tip resistance of CsCl-filled

pipettes used for standard whole cell recordings ranged from 0.5 to 1.5 MΩ. The tip resistance for pipettes used in perforated patch experiments ranged from 1.5 to 2.5 MΩ. At the end of some perforated patch experiments, the membrane patch was intentionally ruptured to measure the difference in access resistance between perforated patch and standard whole cell configurations. In general, access resistance was about threefold higher in the perforated patch than in the whole cell configuration. Membrane capacitance neutralization and, when necessary, series resistance compensation, were optimized. Command potentials were delivered every 15 s, unless otherwise noted. Membrane currents were filtered at 2 kHz (internal Axopatch filter) and digitized at sample intervals of 100–250 μs (Ca^{++} currents) or 1,000 μs (Cl^- currents). Experiments were performed at 22–25°C. In standard whole cell recordings, the measured series resistance (R_s) averaged 2.2 ± 0.1 MΩ (n = 42) with CsCl (135–160 mM)-filled pipettes, and 3.2 ± 0.1 MΩ (n = 59) with *N*-methyl glucamine chloride (NMG-Cl, 130 mM)-filled pipettes.

Perforated Patch Configuration

The perforated patch technique was used to record whole cell membrane currents in the virtual absence of washout and with little disruption of endogenous cellular Ca^{++} buffering mechanisms. Rather than rupturing the membrane patch after gigaseal formation, this technique utilizes the polyene antibiotic, nystatin, to form voltage-insensitive ion pores in the membrane patch under the recording pipette (Horn and Marty, 1988). These pores are somewhat selective for cations over anions (Cass et al., 1970; Marty and Finkelstein, 1975; Horn and Marty, 1988), but are impermeant to Ca^{++}, other multivalent ions, and molecules >0.8 nm in diameter (Holz and Finkelstein, 1970). Briefly, a nystatin stock solution consisting of 50 mg/ml nystatin in DMSO was prepared and stored at −20°C for up to 1 mo. Immediately prior to use, the stock was diluted 500-fold in the pipette solution and ultrasonicated, to give a final nystatin concentration of 100 μg/ml in 0.2% DMSO. This concentration of DMSO, applied to cells studied in the whole cell configuration, had no observable effect on resting membrane conductance, Ca^{++} currents, or Ca^{++} current rundown (unpublished observations). The final nystatin solution remained useful for ~2–3 h, after which fresh final nystatin solutions were prepared from the stock. Gigaseal patches usually could not be obtained with nystatin at the pipette tip. Consequently, after fire-polishing, the tip of the pipette was filled with nystatin-free solution. The pipette was then backfilled with the nystatin-containing solution.

After obtaining the high resistance seal, the pipette potential was set to −60 mV, and voltage pulses (−10 mV amplitude, 20 ms duration) were periodically delivered to monitor the access resistance. As the nystatin diffused to the pipette tip and entered the membrane, the series resistance decreased and a slow capacitive current appeared (Fig. 1 *A*). Access to the cell interior was judged by the first appearance of a capacitive transient; in the cell illustrated in Fig. 1 *A*, access first occurred 4 min after the seal was obtained. When the series resistance dropped below ~60 MΩ, the capacitive transient could be neutralized (Fig. 1 *A*, *bottom trace*), and the series resistance and membrane capacitance could be monitored. The minimum series resistance obtained depended on the nystatin concentration (Fig. 1 *B*); with 100 μg/ml nystatin in the recording pipette, the series resistance fell to an average of 18.9 ± 1.5 MΩ (SEM, n = 38). In typical experiments, the series resistance reached 40 MΩ within 5–20 min and reached a steady level of 10–20 MΩ within 10–40 min after making a seal. We usually began our experiments when the series resistance approached 30 MΩ. The mean measured capacitance with 100 μg/ml nystatin was 11.9 ± 1.2 pF (n = 38), which was not significantly different from that measured in whole cell recordings (11.3 ± 0.3 pF, n = 108). For the largest Cl^- currents and series resistance, the series resistance error approached 7–10 mV. Generally, however, the series resistance error in the reported experiments was <7 mV.

Three observations indicate that the membrane patch was indeed perforated and not ruptured (as in whole cell recording), and that Ca^{++} did not traverse the membrane patch. First, when the pipette was filled with nystatin and the membrane patch was ruptured, either spontaneously or by suction, the cell quickly became leaky and died. Second, several experiments were performed with 5 mM Ca^{++} in the recording pipette as a replacement for Mg^{++}. Had Ca^{++} freely traversed the membrane patch, cells rapidly would have become leaky and died. They didn't. Finally, Ca^{++} currents did not run down in perforated patch recordings, as they did in whole cell recordings (see Results).

Current Measurements

Unless otherwise stated, Ca^{++} current amplitudes were measured 80 ms from the start of a 100-ms voltage step. Ca^{++}-dependent Cl^- tail current amplitudes were measured 2–5 ms

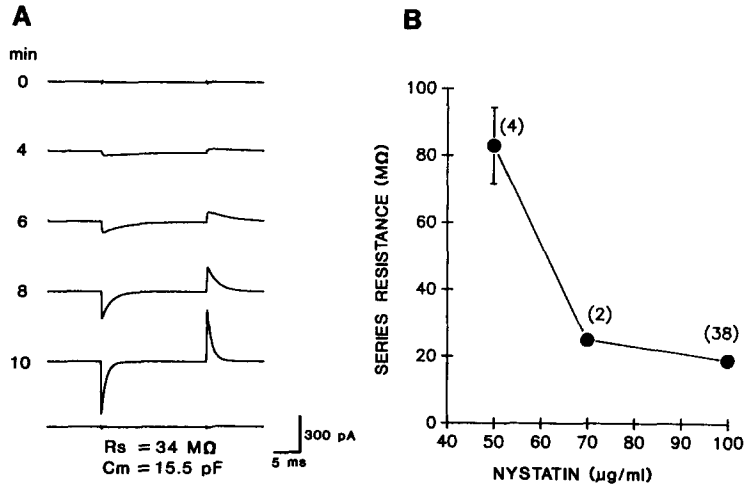

FIGURE 1. Formation of electrical access to the cell interior during perforated patch recordings. (*A*) Traces represent membrane current responses to a 20-ms, −10-mV voltage pulse from a holding potential of −60 mV. Numbers to the left of each trace indicate the time (in minutes) after formation of gigaseal patch. In the bottom trace, the capacitive current was electronically neutralized; series resistance (*Rs*) and cell capacitance (*Cm*) are shown. (*B*) Concentration dependence of the steady-state series resistance on nystatin concentration. Data points represent the mean ± SEM; numbers above the points represent the number of cells included in the mean.

after membrane repolarization, long after the total deactivation of Ca^{++} tail currents (Korn and Weight, 1987). Cl^- tail currents decay with complicated kinetics that vary from cell to cell (Korn and Weight, 1987; see Results). Consequently, the rate of decay could not be consistently fit by the sum of a reasonable number of exponentials. To quantify the tail current decay time course, we measured the tail current duration from peak to 10% of peak (peak to 20% of peak in Fig. 12).

Solutions

The volume of the bathing solution in the recording chamber (35-mm culture dish) was ~1 ml. Experiments were performed both in static and flowing (0.6 ml/min) solutions, with sim-

ilar results. The bathing solution used in all standard whole cell experiments consisted of (in millimolar): 155 NaCl, 5 $CaCl_2$; 10 HEPES and 20 glucose (pH 7.35, osmolality 340). The same bathing solution was used for all perforated patch experiments except that 5 mM KCl was added in place of 5 mM NaCl to maintain Na^+-K^+ ATPase activity. ATPases presumably are nonfunctional in standard whole cell recordings due to washout of ATP. Nonetheless, it is unlikely that intracellular [Na^+] rose in either recording situation, since little or no Na^+ was added to internal solutions, and the Na^+ initially present in the intact cell would rapidly diffuse out through the ruptured membrane patch or nystatin pores during the experiment. The pipette solutions used in standard whole cell recordings contained predominantly either 135–160 mM CsCl or 100–130 mM NMG-Cl, plus 10 mM HEPES. The exact composition of these solutions, which varied according to the requirement of each experiment, is listed in the figure legends. The pipette solution used for all perforated patch experiments consisted of (in millimolar): 55 CsCl; 75 Cs_2SO_4; 5–8 $MgCl_2$ and 10 HEPES (pH 7.35, osmolality 305). The partial substitution of SO_4^{2-} (which does not permeate nystatin pores) for Cl^- reduced the Donnan potential across the membrane patch caused by impermeant, intracellular anions (Horn and Marty, 1988), but retained enough intracellular Cl^- to carry inward Cl^- currents. In earlier experiments, 20 mM glucose, which does not permeate nystatin pores (Holz and Finkelstein, 1970), was included in the pipette solution. Tetrodotoxin (1–5 μM) was included in all bathing solutions (except in the experiment illustrated in Fig. 6 *A*) to block voltage-activated Na^+ channels.

Solution Changes

Solutions surrounding the cell were changed (or drugs applied) by lowering a large bore (30–100 μm) pipette that contained the desired test solution near the cell under study. Application of test solution was terminated by removing the large bore pipette from the bath.

Some experiments (Fig. 10) required a more rapid change in the solution bathing the cell. To effect the rapid change, the large bore pipette was mounted on a holder that was connected to a magnetic stepping device (magnetic coil from relay #A410363732-12, Guardian Electric, Chicago, IL). The pipette containing test solution was lowered into the bath to the vertical plane of the cell, 700 μm downstream from the cell in the flowing bath solution. To apply the test solution, the magnet was switched, and the pipette was stepped horizontally, in a single 700-μm increment, to appose the cell. Reversing the magnetic switch stepped the pipette back to the original position, downstream from the cell in the flowing bath solution. The time constant for the complete cellular response to a change of K^+ solutions bathing the cell ranged from 40–110 ms. Total removal of the test solution after stepping the large bore pipette away from the cell required about 1–4 s, depending on the flow characteristics of the bath.

RESULTS

Ca^{++} Current Rundown

Voltage-activated Ca^{++} currents were studied in GH_3 cells loaded with either Cs^+ (Figs. 2 and 3) or NMG^+ (Fig. 4) to prevent current flow through K^+ channels. In standard whole cell recordings, the amplitude of voltage-activated Ca^{++} currents decreases over time. This "Ca^{++} current rundown" apparently results from washout of intracellular biochemicals that are thought to be involved in Ca^{++} channel phosphorylation and, perhaps, protection of the channel from proteolysis (Chad and Eckert, 1986; Eckert et al., 1986; Belles et al., 1988*a*). The experiments described in this section were designed to compare time-dependent changes in Ca^{++} currents

recorded with standard whole cell and perforated patch techniques. In order to focus on the L-type Ca^{++} channel (see below), we measured Ca^{++} current amplitude at 80 ms after the voltage step to 0 mV.

Voltage pulses (100 ms) from a holding potential of −70 mV to 0 mV were delivered every 15 s, starting within 15–20 s after gaining access to the cell interior. When standard whole cell recording techniques were used, Ca^{++} currents increased in amplitude for the first 1–3 min and then steadily ran down (Fig. 2, *A* and *C*, *diamonds*). After repolarization to −70 mV, a slow inward tail current was often

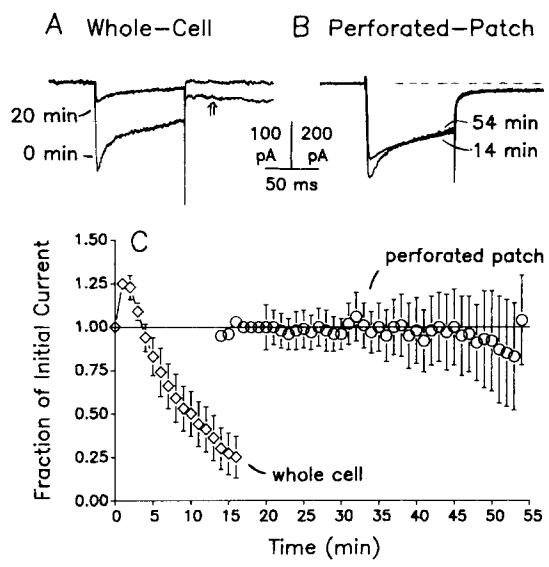

FIGURE 2. Ca^{++} current rundown in GH_3 cells recorded with standard whole cell and perforated patch techniques. Ca^{++} currents were elicited every 15 s by 100-ms voltage steps to 0 mV from a holding potential of −70 mV. (*A*) Ca^{++} currents recorded with the standard whole cell method, elicited 15 s and 20 min after rupture of the membrane patch. Double arrow points to the slow tail current, which disappeared over time concomitant with an increase in leak current (currents were leak-subtracted). (*B*) Ca^{++} currents recorded with the perforated patch method, elicited 14 and 54 min after gaining electrical access to cell. The dashed line indicates zero current level. *Rs* and *Cm* = 9.7 MΩ and 23.2 pF, respectively. (*C*) Time course of Ca^{++} current rundown in a population of cells recorded with each method. Ca^{++} current amplitude was measured 80 ms after the onset of the voltage step; amplitudes in each cell were normalized to the first current recorded (15 s after break-in in standard whole cell recordings). Whole cell currents declined to 50 ± 13% (mean ± SEM, $n = 8$) of the initial current at $t = 10$ min. Perforated patch data represent mean ± SEM for four to five cells at $t = 23$–53 min, one to four cells at other times. Mean *Rs* = 2.18 ± 0.22 MΩ in whole cell recordings, 14.9 ± 2.1 MΩ in perforated patch recordings. The whole cell pipette solution consisted of (in millimolar): 160 CsCl, 10 HEPES, and 0.1 EGTA/Na (pH 7.35, osmolality 307).

evident (Fig. 2 *A*, *double arrow*). In cells not loaded with high [EGTA], GH_3 tail currents disappeared over the course of several minutes, coincident with an increase in leak current of the same amplitude (20–40 pA; traces in Fig. 2 *A* are leak-subtracted). When 10 mM EGTA was added to the pipette solution, the leak current did not develop, and the tail current decreased as the voltage-activated Ca^{++} current ran down. The leak and slow tail currents in GH_3 cells were not carried by Cl^-, and were abolished by substitution of TEA^+ for external Na^+ or Ba^{++} for external Ca^{++} (Korn and Horn, unpublished observations). It appeared, therefore, that the

tail current was Ca^{++} activated, and the slow development of steady leak current resulted from buildup of intracellular Ca^{++}. This tail current was also observed in many perforated patch experiments (Fig. 2 *B*). Whether the GH_3 slow tail current resulted from electrogenic Na^{+}-Ca^{++} exchange or ion channel activation is being investigated.

When the perforated patch technique was used, rundown of voltage-activated Ca^{++} currents was usually negligible for 30–60 min. Fig. 2 *B* illustrates Ca^{++} currents elicited from one cell using the same protocol as in Fig. 2 *A*, recorded 14 and 54 min after gaining access to the cell interior. The average rate of Ca^{++} current rundown in five cells is plotted in Fig. 2 *C* (*circles*). There was considerable variability in the stability of the Ca^{++} current amplitude, as demonstrated by the standard error bars (Fig. 2 *C*, *circles*). In some cells the Ca^{++} current slowly increased in amplitude, in some cells, the current amplitude slowly decreased. In all cases, however, changes in Ca^{++} current amplitude occurred extremely slowly in perforated patch experiments relative to those in standard whole cell experiments. Also during the first 30–60 min of perforated patch recording, there was little or no change in the leak or tail current amplitudes (Fig. 2 *B*). In some cases, after 40–80 min of recording, passive leak currents increased and voltage-activated currents began to run down.

Two Subtypes of Ca^{++} Current in Perforated Patch Recordings

Calcium channels in GH_3 cells come in at least two varieties (Armstrong and Matteson, 1985). Slowly deactivating (SD or T type) calcium channels inactivate relatively quickly (within tens to hundreds of milliseconds) following activation, activate at relatively negative voltages, and are totally inactivated when cells are held at potentials more positive than −50 mV. In contrast, fast deactivating (FD or L type) channels inactivate very slowly, are activated by voltage steps to more positive voltages, and can be studied in the relative absence of T-type channel activity when cells are held at potentials around −40 mV (Armstrong and Matteson, 1985; Bean, 1985; Hess et al., 1986). Both channel types were maintained in perforated patch recordings from GH_3 cells. Fig. 3, for example, shows Ca^{++} currents from a perforated patch experiment recorded 2.5 h after gaining electrical access to the cell interior. Figs. 3, *A* and *B*, illustrate Ca^{++} currents elicited from holding potentials of −90 and −40 mV. As observed in studies which utilized the standard whole cell recording technique (Bean, 1985; Armstrong and Matteson, 1985; DeRiemer and Sakmann, 1986), cells held at −90 mV displayed an early transient Ca^{++} current followed by a sustained Ca^{++} current. In contrast, cells held at −40 mV did not display an early transient current. In Fig. 3 *C*, currents elicited by steps to ~0 mV from each holding potential are superimposed for comparison. In this cell, the L-type current constituted ~70% of the peak current at 0 mV. The voltage range of Ca^{++} current activation (Fig. 3 *D*) was also consistent with that observed in previous whole cell studies (Dubinsky and Oxford, 1984; Bean, 1985; DeRiemer and Sakmann, 1986). Ca^{++} currents were largest after steps to ~ +10 mV, and activated at more negative potentials when cells were held at −90 mV (Fig. 3 *D*, *filled circles*) than when they were held at −40 mV (Fig. 3 *D*, *open circles*).

Influence of Na^+-Ca^{++} Exchange on Ca^{++} Current Rundown

Ca^{++} current rundown appears to be at least partially dependent on intracellular Ca^{++} (Byerly and Hagiwara, 1982; Fenwick et al., 1982; Forscher and Oxford, 1985; Eckert et al., 1986; Belles et al., 1988*a*, *b*). The experiments described in this section tested whether inhibition of Na^+-Ca^{++} exchange facilitated Ca^{++} current rundown in cells recorded with the standard whole cell method, and whether inhibition of Na^+-Ca^{++} exchange caused rundown in cells recorded with the perforated patch method. Na^+-Ca^{++} exchange was inhibited by replacement of extracellular Na^+ with tetraethylammonium (TEA^+) or tetramethylammonium (TMA^+). The specificity of action of these Na^+ substitutes is addressed below.

In standard whole cell recordings, the influence of Na^+-Ca^{++} exchange on Ca^{++} current rundown depended on the concentration of EGTA in the recording solu-

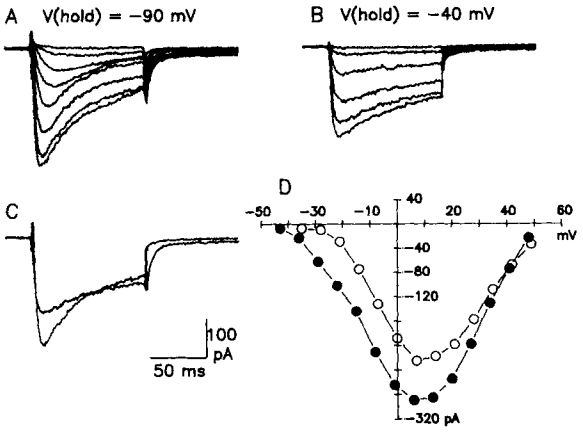

FIGURE 3. Voltage - activated Ca^{++} currents recorded from a Cs^+-loaded GH_3 cell, using perforated patch method. (*A*) The holding potential was −90 mV. Ca^{++} currents were activated by 100-ms voltage steps to potentials ranging from −43 to +6 mV, in 7-mV increments. (*B*) The holding potential was −40 mV. Currents were activated by steps ranging from −28 to +7 mV, in 7-mV increments. (*C*) A current activated by a step from −90 to −1 mV is superimposed on a current activated by a step from −40 to 0 mV. *Rs* = 12 MΩ, *Rs* compensation = 80%. Currents were filtered at 2 kHz (−3 dB) during acquisition, and digitally filtered at 500 Hz for display. (*D*) Ca^{++} *I-V* relationships for holding potentials of −90 mV (*filled circles*) and −40 mV (*open circles*). Current amplitudes were measured at the peak.

tion (Fig. 4). With only 0.1 mM EGTA in the recording solution, replacement of extracellular Na^+ with TEA^+ accelerated Ca^{++} current rundown (Fig. 4, *A* and *C*). 5 min after gaining access to the cell interior, Ca^{++} current amplitudes in cells recorded in extracellular Na^+ were 101 ± 4% (SEM, n = 8) of control. In contrast, when extracellular Na^+ was replaced by TEA^+ 30–45 s after gaining access to the cell interior, Ca^{++} current amplitudes declined to 33 ± 9% (n = 7) of control in 5 min. This acceleration of rundown by Na^+ substitution was not observed when the recording solution contained 10 mM EGTA (Fig. 4 *D*), which suggests that the effects of Na^+ substitution on rundown required changes in internal [Ca^{++}]. Acceleration of rundown could not have been due to reversal of the Na^+-Ca^{++} exchange mechanism, since there was no internal Na^+ to run the exchanger in the reverse direction. An additional effect of Na^+ substitution by TEA^+ was an increase in Ca^{++} current amplitude (Fig. 4 *B*). However, the increase in Ca^{++} entry could not

account for the effects of Na^+ substitution on rundown. Ca^{++} current potentiation, but not acceleration of rundown, occurred even with high intracellular [EGTA], and the rate of rundown was greater in TEA even when Ca^{++} currents were smaller (Fig. 4 *C*).

The results in Fig. 4 indicate that Ca^{++} current rundown in GH_3 cells has a large Ca^{++}-dependent component, and that Na^+-Ca^{++} exchange is an important Ca^{++} clearance mechanism in standard whole cell recordings. However, these results reflect the influence of the exchanger under artificial intracellular Ca^{++} buffering condition, and not under conditions in which the cell's natural buffering mechanisms are entirely responsible for Ca^{++} clearance. To retain endogenous cellular buffering mechanisms, we used the perforated patch technique, in which Ca^{++} did

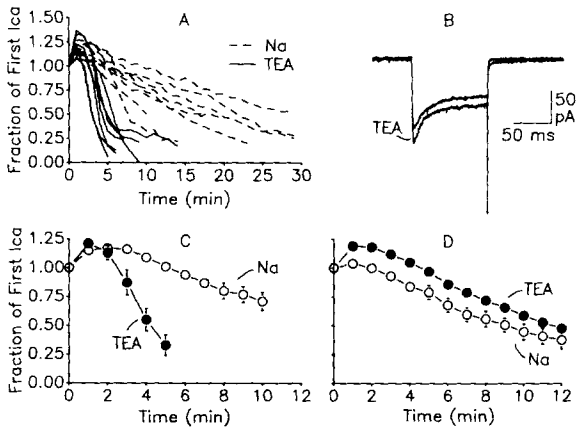

FIGURE 4. Facilitation of Ca^{++} current rundown in standard whole cell experiments by inhibition of Na^+-Ca^{++} exchange. Ca^{++} currents were elicited as in Fig. 3. (*A*) Time course of Ca^{++} current rundown in GH_3 cells, perfused internally with a low [EGTA], in the presence of extracellular Na^+ (eight cells, *dashed lines*) or after total replacement of extracellular Na^+ with TEA^+ (seven cells, *solid lines*). In the latter experiments, Ca^{++} currents were initially recorded in extracellular Na^+ for 30 or 45 s (two or three stimuli); the cells were then bathed continuously in TEA^+ for the remaining time. *Rs* = 3.19 ± 0.43 MΩ (Na^+) and 3.21 ± 0.71 MΩ (TEA^+). (*B*) Ca^{++} currents elicited before (unlabeled) and within 15 s of switching from Na^+ to TEA^+ solutions. The recording pipette contained 10 mM EGTA. (*C*) Time course of Ca^{++} current rundown, averaged from data illustrated in *A*. (*D*) Same experiment as in *C*, except that cells were perfused internally with a high [EGTA]. Points represent mean ± SEM of seven cells in each condition. *Rs* = 3.22 ± 0.27 MΩ (Na^+) and 4.51 ± 0.61 MΩ (TEA^+). Pipette solution in *A* and *C* (in millimolar): 130 *N*-methyl glucamine (NMG)-Cl, 10 CsCl, 5 TEA-Cl, 10 HEPES, 0.1 EGTA/Na, and 20 sucrose. Pipette solution in *B* and *D* (in millimolar): 130 NMG-Cl, 10 HEPES, 11 EGTA/Na, 1 $CaCl_2$, and 20 sucrose.

not escape from the cell via the recording pipette, and ATP-dependent pumps and phosphorylating systems presumably still operated (as evidenced by the lack of Ca^{++} current rundown). In contrast to results obtained with the standard whole cell technique, substitution of extracellular TEA^+ for Na^+ in the first 30 min of perforated patch recordings did not facilitate Ca^{++} current rundown (Fig. 5). These data indicate that, for at least 30 min, a functional Na^+-Ca^{++} exchange system is not necessary to protect cells from a loss of Ca^{++} channel function.

Ca^{++}-activated Cl^- Currents

In Cs^+-loaded AtT-20 cells studied with standard whole cell recording methods, step depolarization activates both a voltage-activated Ca^{++} current and a Ca^{++}-depen-

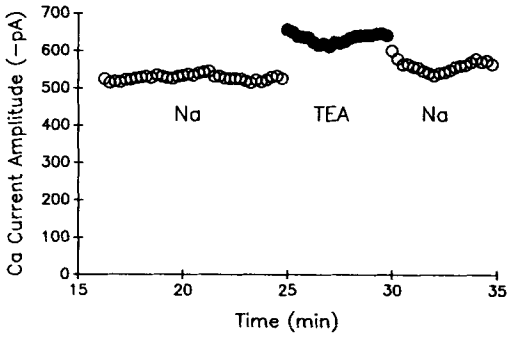

FIGURE 5. Lack of current Ca^{++} current rundown in GH_3 cells with the perforated patch method, even after inhibition of Na^+-Ca^{++} exchange. Ca^{++} currents were elicited as in Fig. 4, except that the perforated patch technique was used. Similar data were obtained in each of two cells, in which the switch from extracellular Na^+ (*open circles*) to TEA^+ (*filled circles*) did not facilitate Ca^{++} current rundowns. *Rs* = 23 MΩ.

dent Cl^- current (Fig. 6 *A*, see Fig. 7 *A* for example of voltage step protocol). After repolarization, the Ca^{++} current deactivates within ~0.4 ms and a slow, apparently pure Ca^{++}-dependent Cl^- tail current is observed (Korn and Weight, 1987). As long as the Cl^- channel current does not reach saturation, the amplitude of the tail current at a given repolarization potential provides a qualitative measure of Ca^{++} current amplitude during the voltage step (Korn and Weight, 1987). Furthermore, since these Cl^- channels show little or no inactivation, the time course of current deactivation at a given repolarization potential provides a measure of the time course of $[Ca^{++}]$ decline near the Cl^- channel (Korn and Weight, 1987). The experiments in this section were designed to examine the stability of Ca^{++}-activated Cl^-

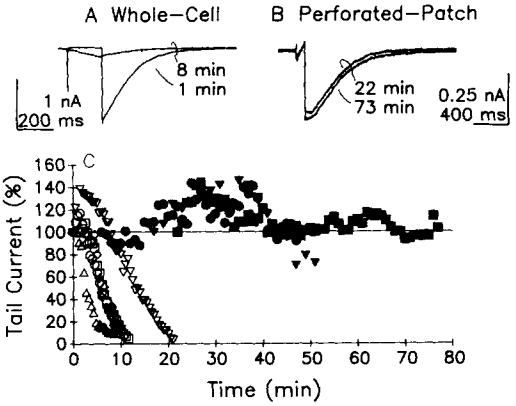

FIGURE 6. Rundown of Ca^{++}-dependent Cl^- current in AtT-20 cells recorded with standard whole cell and perforated patch techniques. (*A*) Ca^{++}-dependent Cl^- currents recorded with standard whole cell method, elicited 1 and 8 min after rupture of the membrane patch. Currents were elicited with a 200-ms voltage pulse to 0 mV from a holding potential of −70 mV. *Rs* = 1.6 MΩ. (*B*) Ca^{++}-dependent Cl^- currents recorded with the perforated patch method, 22 and 73 min after gaining electrical access to the cell interior. Currents were elicited with a 100-ms voltage pulse to +5 mV from a holding potential of −70 mV. *Rs* = 26.5 MΩ. (*C*) Rundown of Ca^{++}-activated Cl^- tail currents in five cells recorded with the whole cell technique (*open symbols; Rs* = 2.64 ± 0.19 MΩ) and in three cells recorded with the perforated patch technique (*filled symbols; Rs* = 14.1 ± 5.1 MΩ). Tail current amplitudes were measured 5 ms after repolarization, and normalized to the amplitude of the initial tail current. The whole cell pipette solution contained (in millimolar): 135 CsCl, 10 HEPES, 0.1 EGTA/Na, and 20 sucrose (pH 7.35, osmolality 307). TTX was omitted in the experiment in *A* in order to simultaneously monitor voltage-activated Na^+ currents during the rundown of the Ca^{++}-activated Cl^- current. Na^+ current amplitude remained unchanged during Cl^- current rundown.

currents and the stability of intracellular Ca^{++} buffering near the plasma membrane in perforated patch recordings.

In standard whole cell recordings, Ca^{++}-dependent Cl^- currents in AtT-20 cells ran down with a time course similar to that of Ca^{++} currents in GH_3 cells (Fig. 6, *A* and *C*, *open symbols*). Cl^- currents reached 50% of their initial amplitude in 7 ± 2.1 min (SEM, $n = 5$). As with Ca^{++} currents, Cl^- current rundown was prevented by use of the perforated patch technique (Fig. 6, *B* and *C*, *closed symbols*). Not only did the magnitude of the Ca^{++}-activated Cl^- current remain relatively stable, but the time course of Cl^- current decay also remained relatively unchanged (Fig. 6 *B*). This

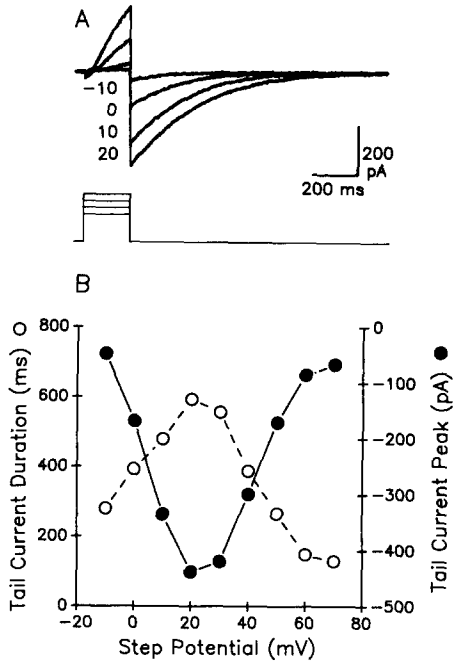

FIGURE 7. Relationship between tail current amplitude, tail current duration, and activation potential in perforated patch recordings of AtT-20 cells. Ca^{++}-dependent Cl^- currents were activated by 200-ms voltage steps from a holding potential of −70 mV. (*A*) Currents elicited by voltage steps to the potentials indicated. The lower traces illustrate the stimulus protocol. *Rs* = 16 MΩ. (*B*) Plot of tail current duration (time from peak to 10% of peak) and tail current amplitude (measured 5 ms after repolarization) as a function of step potential.

suggests that the mechanisms involved in the clearance of intracellular Ca^{++} from the cytoplasmic face of the plasma membrane remained stable.

In previous whole cell experiments in which no exogenous Ca^{++} buffer was added to the pipette solution, the Cl^- tail current decayed nonexponentially, occasionally increased briefly immediately after repolarization, and decayed with a time course that was closely correlated with the amplitude of the voltage-activated Ca^{++} current (Korn and Weight, 1987). Addition of 200 μM intracellular EGTA resulted in tail currents that often decayed exponentially, with durations that were independent of the Ca^{++} current amplitude (Korn and Weight, 1987). Addition of 10 mM EGTA totally prevented current activation.

In perforated patch recordings, the decay kinetics of the Ca^{++}-activated Cl^- current were qualitatively similar to those of standard whole cell recordings performed without exogenously added Ca^{++} buffer. The tail current did not decay exponen-

tially (Figs. 6 *B*, 7 *A*, 8), and often decayed with complex kinetics (Fig. 6 *B*). As in standard whole cell recordings (Korn and Weight, 1987), the Cl^- tail current amplitude for given step and repolarization potentials (Fig. 7 *B*, *filled circles*) reflected the Ca^{++} current amplitude for that voltage step. Furthermore, the tail current duration (Fig. 7 *B*, *open circles*) was closely correlated to the tail current amplitude (Fig. 7 *B*, *filled circles*). This correlation suggests that the tail current decay rate was dependent on the amount of Ca^{++} that entered during a stimulus, and the rate at which Ca^{++} left the vicinity of the Cl^- channels. Experiments described below (Fig. 12) demonstrate that Cl^- tail currents decay much faster (decay time constant <100 ms) when intracellular [Ca^{++}] is fixed, and Cl^- channels are activated by voltage. Together, these observations implicate Ca^{++} buffering mechanisms near the plasma membrane as important regulators of Cl^- current duration. The experiments in the next section address this hypothesis.

Effect of Na^+-Ca^{++} Exchange on Ca^{++}-dependent Cl^- Currents

In perforated patch experiments, as in standard whole cell experiments (Korn and Weight, 1987), substitution of TMA^+ or TEA^+ for extracellular Na^+ prolonged and

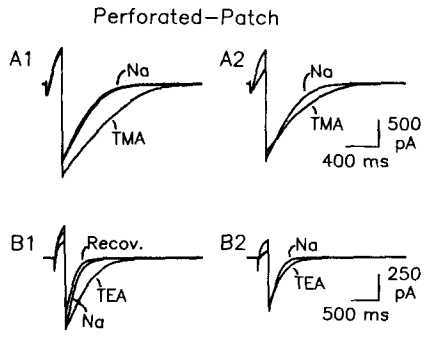

FIGURE 8. Prolongation of Ca^{++}-activated Cl^- currents in AtT-20 cells by substitution of TMA^+ or TEA^+ for extracellular Na^+. Perforated patch recordings of Ca^{++}-activated Cl^- currents in the presence of extracellular Na^+ and after replacing Na^+ with either TMA^+ (*A*) or TEA^+ (*B*). (*A1*) Currents were elicited by 200-ms voltage steps to +15 mV from a holding potential of −70 mV. The two superimposed current traces labeled "*Na*" consist of one trace each from control and recovery. (*A2*) Comparison of currents elicited by voltage steps to +15 mV (Na) and +5 mV (TMA). (*B1*) Currents were elicited by 200-ms voltage steps to +10 mV from a holding potential of −60 mV. Trace labeled "*Recov.*" was elicited after return to Na^+-containing solution. (*B2*) Comparison of currents elicited by voltage steps to +10 mV (Na) and 0 mV (TEA). *Rs* = 15.2 MΩ (*A*) and 31 MΩ (*B*).

potentiated the Ca^+-dependent Cl^- current (Fig. 8). Both effects were reversible upon return to Na^+.

Since the tail current duration was positively correlated with tail current amplitude, and both Ca^{++} and Cl^- currents were potentiated by Na^+ substitution (Figs. 4 *B*, 8, *A1*, and *B1*), it was possible that the increased Cl^- current duration following Na^+ substitution was due simply to increased Ca^{++} entry during the voltage step. Four observations indicate that this was not the case. First, Na^+ substitution changed the rate of Cl^- current decay, so that tail currents in the presence of a Na^+ substitute decayed more slowly even at a poststimulus time when they were smaller (reflecting a lower local [Ca^{++}]) (Fig. 8). Second, tail currents elicited in the presence of Na^+ were compared with those elicited in the presence of TMA^+ or TEA^+

that were closely matched in initial amplitude (Fig. 8, *A2* and *B2*). This match was accomplished by comparing currents elicited by steps to different voltages. Tail currents in the presence of TMA^+ or TEA^+ were prolonged relative to those in Na^+-containing solutions, even when tail currents in Na^+-containing solutions were slightly larger (reflecting slightly greater initial Ca^{++} load). Third, tail currents were prolonged by exchanging TEA^+ for Na^+ even when TEA^+ was applied during the tail current decay phase, hundreds of milliseconds after the Ca^{++} had ceased (see Fig. 10 *A* below). Finally, in standard whole cell experiments, TEA^+- and TMA^+-induced tail current prolongation was prevented by the addition of at least 0.2 mM intracellular EGTA, whereas under these same conditions, potentiation of Ca^{++} and Cl^- currents still occurred (Fig. 4 *B*; Korn and Weight, 1987). These data suggest that Cl^- tail current prolongation was due to an alteration in intracellular Ca^{++} buffering, and not simply to an increased influx of Ca^{++}. In contrast, it appears that Cl^- current potentiation following Na^+ substitution by TEA^+ and TMA^+ was due at least partly to the potentiation of voltage-activated Ca^{++} currents (but see also Fig. 12).

The Ca^{++} Dependence of the Influence of Na^+-Ca^{++} Exchange

We also examined the influence of Na^+-Ca^{++} exchange on the duration of Ca^{++}-activated Cl^- currents as a function of tail current amplitude (Fig. 9). Tail current amplitude was varied by varying Ca^{++} influx during the voltage step, and was thus a measure of Ca^{++} influx. Ca^{++} influx was varied by stepping the membrane potential to a fixed voltage for sequentially increasing durations, or by stepping the membrane potential to different voltages for a fixed duration. Similar results were obtained with each protocol. Fig. 9 *A* illustrates Cl^- currents nearly matched for initial amplitude, elicited by fixed duration voltage steps in Na^+- and TMA^+-containing solutions. Na^+ substitution decreased the rate of decay of relatively large tail currents, produced by larger Ca^{++} currents (Fig. 9 *A2*). In contast, the rate of decay of small tail currents, produced by small Ca^{++} currents, was virtually unaffected by Na^+ substitution. In Fig. 9 *B*, tail current duration is plotted as a function of tail current amplitude for families of Cl^- currents elicited in Na^+-containing and Na^+-free solutions. Two points can be made from this plot. First, at any given initial tail current amplitude (amount of Ca^{++} influx), current duration was longer in TMA^+ than in Na^+. Second, the steeper relationship between current amplitude and duration in TMA^+ indicates that Na^+ substitution influenced current duration more as Ca^{++} influx became greater.

Direct vs. Homeostatic Involvement of Na^+-Ca^{++} Exchange

Two fundamentally different mechanisms could have been responsible for the prolongation of Ca^{++}-dependent Cl^- currents following blockade of Na^+-Ca^{++} exchange. First, Na^+-Ca^{++} exchange might directly influence the $[Ca^{++}]$ near the Cl^- channel after a Ca^{++} transient. Inhibition of the exchanger would slow the removal of Ca^{++}, and consequently prolong the Ca^{++}-dependent Cl^- current. This hypothesis predicts that the prolongation after blockade of Na^+-Ca^{++} exchange would be immediate.

Alternatively, Na^+-Ca^{++} exchange might play a role in extruding Ca^{++} from the

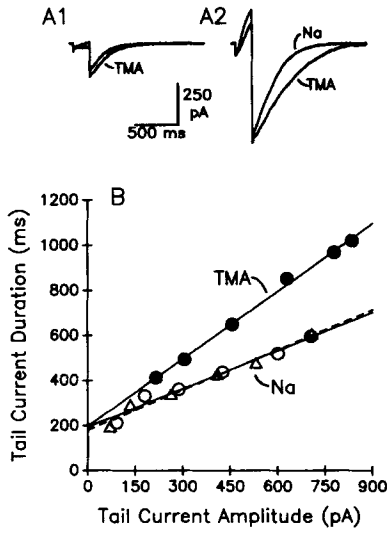

FIGURE 9. Influence of Na^+-Ca^{++} exchange depended on the amplitude of the Ca^{++}-activated Cl^- current in AtT-20 cells. (*A1*) Currents were elicited by 200-ms voltage steps to −5 mV in extracellular Na^+ (unlabeled trace) and −10 mV after the switch to TMA^+, from a holding potential of −70 mV. (*A2*) Currents were elicited by voltage steps to +10 mV (Na) and +5 mV (TMA). (*B*) Tail current duration (measured from peak to 10% of peak) as a function of tail current amplitude (measured 5 ms after repolarization). Control (*open circles, solid line*) and recovery (*open triangles, dashed line*) data sets were obtained with extracellular Na. *Rs* = 15.2 MΩ.

cell, but not be involved in the regulation of transient [Ca^{++}] changes near the plasma membrane. The primary responsibility for buffering Ca^{++} transients might belong to other Ca^{++} buffering mechanisms. The lack of Ca^{++} extrusion due to inhibition of Na^+-Ca^{++} exchange might then result in a buildup of intracellular Ca^{++}, which would eventually saturate the buffers that normally regulate [Ca^{++}] transients, and would thereby prolong Ca^{++}-dependent currents. This hypothesis predicts that, after blockade of Na^+-Ca^{++} exchange, prolongation of Ca^{++}-dependent currents would be delayed, and that currents would progressively become more prolonged, as the other buffering mechanisms became saturated.

The experiments illustrated in Fig. 10 strongly support the first hypothesis. A magnetically driven apparatus was used to rapidly change the solution bathing the cell (see Methods). In the first experiment, the solution was changed during the decay phase of the Ca^{++}-dependent Cl^- current (Fig. 10 *A*, see arrow). The rate of Cl^- current decay changed within several tens of milliseconds of switching from Na^+-containing to TEA^+-containing solutions (see arrow). In the second experiment, stimuli were presented to elicit Cl^- currents every 30 s and the bathing solu-

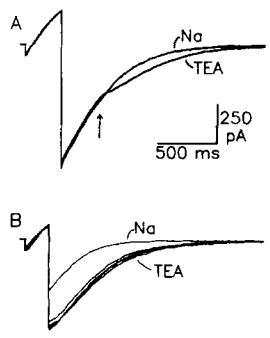

FIGURE 10. Latency to prolongation of Ca^{++}-dependent Cl^- current after inhibition of Na^+-Ca^{++} exchange. (*A*) Two currents, elicited by 300-ms voltage steps to +5 mV from a holding potential of −70 mV. During the decay phase of the second tail current (at the arrow), the bathing solution was rapidly switched from a Na^+-containing solution to one containing TEA^+ (see Methods). (*B*) Currents elicited by 200-ms voltage steps to +5 mV in extracellular Na^+ and 1, 31, 61, and 91 s after switching to extracellular TEA^+. *Rs* = 15 MΩ.

tion was changed ~1 s before the second stimulus. As illustrated in Fig. 10 *B*, the change in Cl^- current time course was complete within 1 s after inhibition of Na^+-Ca^{++} exchange.

Selectivity of Na^+ Substitution by TEA^+

In addition to inhibition of Na^+-Ca^{++} exchange, two alternative mechanisms could account for the effects of Na^+ substitution on the duration of Ca^{++}-dependent Cl^- currents. First, removal of extracellular Na^+ would block Na^+-H^+ exchange, which could result in a buildup of intracellular H^+, which in turn might interfere with intracellular Ca^{++} buffering mechanisms. Second, either Na^+ removal or Na^+ substitutes might slow the kinetics of the Ca^{++}-dependent Cl^- channel via a direct interaction with the channel. The experiments described in Figs. 11 and 12 address these two possibilities, respectively.

To test whether inhibition of Na^+-H^+ exchange was indirectly responsible for the effects of Na^+ substitution on the Ca^{++}-dependent Cl^- current time course, the Cl^-

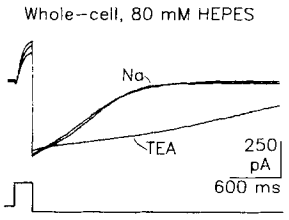

FIGURE 11. TEA^+ does not prolong Cl^- current due to block of sodium-proton exchange. Ca^{++}-dependent Cl^- currents (*top traces*) were recorded with the standard whole cell technique, with 80 mM HEPES in the pipette solution to buffer intracellular pH. Currents were elicited by 200-ms voltage steps to +20 mV from a holding potential of −70 mV; the repolarization potential was −80 mV (*lower trace*). The pipette solution contained (in millimolar): 100 NMG-Cl, 80 HEPES, and 40 Cs^+ (pH 7.34, osmolality 308). Tail currents marked "*Na*" were recorded in Na-containing extracellular solution before and after recovery from replacement of extracellular Na^+ with TEA^+.

current was examined in standard whole cell recordings in which 80 mM HEPES was included in the recording solution (Fig. 11). Substitution of TEA^+ for extracellular Na^+ reversibly prolonged the Ca^{++}-dependent Cl^- current under these conditions of strong intracellular pH buffering. Together with the observation that inclusion of 200 μM EGTA in the recording solution prevents the tail current prolongation by Na^+ substitution (Korn and Weight, 1987), these data are consistent with the conclusion that the prolongation resulted from a change in buffering of intracellular Ca^{++}, but not H^+, after Na^+ substitution.

The experiment in Fig. 12 examined the possibility that the prolongation of the Ca^{++}-dependent Cl^- current by Na^+ substitution was due to a direct effect of TEA^+ on the Cl^- channel, or to sensitivity of the Cl^- channel to removal of extracellular Na^+. The effects of TEA^+ on Cl^- current duration were examined under conditions where intracellular [Ca^{++}] was fixed, influx of extracellular Ca^{++} was prevented, and blockade of Na^+-Ca^{++} exchange would not influence the intracellular [Ca^{++}]. Under these conditions, activation of the Cl^- current is mildly voltage

dependent, with strong depolarization increasing the probability of the channel being open (Evans and Marty, 1986). The intracellular recording solution contained Ca^{++} and Mg^{++} buffered with 10 mM EGTA to concentrations of 1.5 μM and 9.44 mM, respectively. Extracellular Ca^{++} was totally replaced by Mg^{++} to prevent influx of Ca^{++} during voltage steps. The Ca^{++}-dependent Cl^- current was then activated by 800-ms depolarizing voltage steps to +80 mV from the holding potential of −80 mV (Fig. 12). Repolarization reveals an inward tail current that is eliminated by substitution of SO_4^{2-} for Cl^- or by reduction of intracellular [Ca^{++}] (Korn and Weight, 1987). The reversal potential for this tail current (−2 mV) was near the Cl^- equilibrium potential (−5 mV) and was unaffected by the intracellular or extracellular monovalent cations used (Fig. 12, *A* and *C*). Based on its dependence on voltage, Cl^- and Ca^{++}, and the insensitivity of its reversal potential to monovalent cations, this tail current is identified as the Ca^{++}-dependent Cl^- current. Substitution of

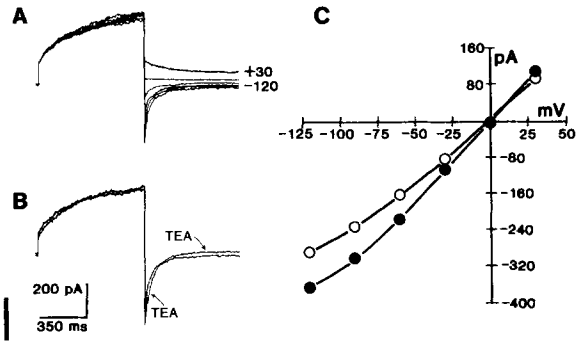

FIGURE 12. TEA^+ does not slow Ca^{++}-dependent Cl^- channel kinetics in the presence of fixed intracellular [Ca^{++}]. Standard whole cell recordings of Ca^+-activated Cl^- currents elicited by 800-ms voltage steps to +80 mV from a holding potential of −80 mV. (*A*) Repolarization to voltages between −120 and +30 mV in 30-mV increments. (*B*) Tail current observed after repolarization to −120 mV, in the presence of extracellular Na^+ (unlabeled) and TEA^+. (*C*) Tail current *I-V* relationship, taken from traces in *A* (extracellular Na^+, *open circles*) and following identical protocol in extracellular TEA^+ (*filled circles*). Tail current was measured 2 ms after repolarization. External solution (in millimolar): 145 NaCl, 10 $MgCl_2$, 10 HEPES, and 20 glucose (pH 7.36, osmolality 335). Pipette solution (in millimolar): 100 NMG-Cl, 10 $MgCl_2$, 7.64 $CaCl_2$, 10 EGTA, 10, HEPES, and 20 sucrose (pH 7.05, osmolality 310). The calculated free internal [Ca^{++}] = 1.5 μM. *Rs* = 4.8 MΩ.

TEA^+ for extracellular Na^+ potentiated but did not prolong the Ca^{++}-activated Cl^- tail current (Fig. 12 *B*); at repolarization potentials between −120 and −30 mV, the tail current duration from peak to 20% of peak was decreased by 4–31% after Na^+ substitution. These data strongly suggest that the tail current prolongation observed in Figs. 8, 10, and 11 was not due to a direct action of TEA^+ application or Na^+ removal on the Cl^- channel.

DISCUSSION

The main findings of this study are (*a*) that rundown of Ca^{++} and Ca^{++}-dependent currents in patch-clamp studies can be prevented by use of the perforated patch technique, (*b*) that removal of free intracellular Ca^{++} by Na^+-Ca^{++} exchange directly contributes to the decay time course of the Ca^{++}-dependent Cl^- current in

pituitary cells, and (*c*) that mechanisms other than Na^+-Ca^{++} exchange also buffer or remove free Ca^{++} on a time scale that is relevant to Ca^{++}-activated currents. Further, these studies suggest that, in contrast to standard whole cell recording, the perforated patch technique permits patch-clamp studies while maintaining phosphorylation mechanisms and preventing unwanted intracellular proteolytic activity.

Ca^{++} Current Washout

Two hypotheses are currently postulated to explain Ca^{++} current rundown during standard whole cell recordings: (*a*) that Ca^{++} channels must be phosphorylated to remain functional and that, during standard recordings, one or more substances necessary for channel phosphorylation wash out (cf. Chad and Eckert, 1986) and (*b*) that during standard whole cell recordings, Ca^{++} channel function is diminished due to proteolytic degradation (Belles et al., 1988*a*; Chad and Eckert, 1986; Eckert et al., 1986). Indeed, it appears that both of these mechanisms may contribute to Ca^{++} current rundown, since addition to the intracellular recording solution of both protease inhibitors and phosphorylating substances together are more effective at preventing rundown than the addition of either one alone (Chad and Eckert, 1986). Both mechanisms are thought to be Ca^{++} dependent, since increasing intracellular Ca^{++} increases the rate of Ca^{++} current rundown and perfusion with high concentrations of EGTA slows the rate of rundown (Byerly and Hagiwara, 1982; Fenwick et al., 1982; Forscher and Oxford, 1985; Belles et al., 1988*b*). Our data (Fig. 4) support the hypothesis that rundown is Ca^{++} dependent.

The observation that rundown is prevented by use of the perforated patch technique has several implications. Typically, rundown is retarded or prevented by the addition to the intracellular recording solution of exogenous substances that support channel phosphorylation, protect against proteolysis, and perhaps act via other unelucidated mechanisms. These substances include EGTA, Mg-ATP, cAMP, cAMP-dependent protein kinase, creatine phosphate, creatine kinase, and the protease inhibitors leupeptin or calpstatin (Doroshenko et al., 1982, 1984; Forscher and Oxford, 1985; Armstrong and Eckert, 1987; Belles et al., 1988 *a*, *b*). A potential problem with this strategy is that these substances may contribute to, saturate, or disrupt biochemical processes involved in the modulation of electrophysiological mechanisms being studied. However, if these substances are not added, experiments must often be interpreted in light of diminishing Ca^{++} channel function, and the possibility that important intracellular biochemicals are washing out of the cell. The perforated patch method allows whole cell studies of Ca^{++} channel function without rundown, without addition of exogenous bioactive substances, and presumably without loss of important endogenous substances. Finally, if Ca^{++} channels are indeed degraded by proteolysis during standard whole cell recordings, it is likely that other proteins may also undergo degradation. The absence of rundown in perforated patch studies suggests that, with this method, such unwanted proteolysis is minimized.

Ca^{++} Buffering in Pituitary Cells

Clearance of free intracellular Ca^{++} in pituitary cells is accomplished by several mechanisms, which include extrusion across the plasma membrane via both a Na^+-

Ca^{++} exchanger and a Ca^{++}-pumping ATPase (Barros and Kaczorowski, 1984; Kaczorowski et al., 1984). By analogy with other cell types, Ca^{++} in pituitary cells may also be buffered by sequestration into organelles such as mitochondria (Chapman, 1986), endoplasmic reticulum (Blaustein et al., 1978; Henkart et al., 1978), and binding to intracellular Ca^{++}-binding proteins (Barish and Thompson, 1983). Finally, simple diffusion of Ca^{++} away from the cytoplasmic membrane surface into the cell interior may be an important mechanism for removal of Ca^{++} from near Ca^{++}-dependent membrane-bound proteins, such as ion channels (cf. Connor and Nikolakopoulou, 1982). One advantage of the perforated patch technique over standard whole cell techniques is the ability to study cells with relatively intact endogenous Ca^{++} buffering mechanisms (see below). This technique permits patch-clamp studies of the roles and modulation of different Ca^{++} buffering mechanisms, and provides a more realistic electrophysiological model of cellular events that depend on transient changes in intracellular [Ca^{++}].

One goal of this study was to determine whether Na^+-Ca^{++} exchange played a direct role in buffering Ca^{++} transients near the plasma membrane, or whether it was involved only in the steady maintenance of low intracellular [Ca^{++}]. We have demonstrated that, in cells studied with the perforated patch technique, Na^+-Ca^{++} exchange plays a significant but nonexclusive role in removing Ca^{++} during the time course of a Ca^{++}-dependent membrane current. The short latency and nonprogressive nature of the Cl^- current prolongation after Na^+ substitution (Fig. 10) strongly suggest that Na^+-Ca^{++} exchange directly removed free Ca^{++} from the region near the Cl^- channels.

Several observations suggest that Na^+-Ca^{++} exchange is just one of several important mechanisms by which Ca^{++} transients near the cytoplasmic surface of the plasma membrane are buffered: (*a*) at all Ca^{++} loads examined, larger Ca^{++} loads resulted in slower tail currents (Fig. 9 *B, open symbols*), which suggests the saturation of process(es) that remove Ca^{++} from near the membrane surface, (*b*) after inhibition of Na^+-Ca^{++} exchange, the dependence of tail current duration on Ca^{++} load became steeper (Fig. 9 *B, filled circles*), which suggests that the remaining Ca^{++} removal mechanisms were saturated to a greater degree at similar Ca^{++} loads, and (*c*) the complicated tail current decay kinetics in the absence of Na^+-Ca^{++} exchange suggests that more than one other mechanism is also involved in the dynamic removal of Ca^{++} from near the membrane surface. Investigation of the functional significance of other mechanisms, which include extrusion by the Ca^{++} ATPase, Ca^{++} sequestration by intracellular organelles, and simple diffusion of Ca^{++} away from the plasma membrane, is currently hampered by the lack of experimental tools that selectively modify each of these physiological processes.

The applicability of these findings to the intact cell relies on the assumption that the relative role of each Ca^{++} buffering mechanism in the studied cells is similar to that of intact cells. While we have no direct evidence from these studies, several indirect lines of evidence suggest that other Ca^{++} buffering mechanisms were still functional. In perforated patch studies, no exogenous Ca^{++} buffers were added to the cell, and no endogenous buffers, such as Ca^{++} binding proteins, could leave. In contrast to standard whole cell recording situations, Ca^{++} could not simply diffuse out of the cell through the membrane patch, and diffusion within the cell interior

would be expected to be more realistic since there is less disruption of the cytoplasm. Ca^{++}-dependent Cl^- currents were only modestly prolonged by inhibition of Na^+-Ca^{++} exchange. Since Ca^{++}-dependent Cl^- currents remain activated in the presence of high intracellular Ca^{++} (Korn and Weight, 1987), other Ca^{++} removal mechanisms must still have been operating. This is further supported by the observation that Ca^{++}-dependent leak currents did not develop in perforated patch studies, even after inhibition of Na^+-Ca^{++} exchange. Finally, since both Ca^{++} channel function and the Ca^{++}-pumping ATPase depend on a supply of Mg^{++} and ATP, and Ca^{++} channel currents did not run down, it is likely that the ATPase also remained functional.

Whereas pituitary cells in vivo live at a temperature of 37°C, the experiments in this study were carried out at room temperature. This does not, however, change the qualitative findings of this study. Both Na^+-Ca^{++} exchange and the Ca^{++}-pumping ATPase operate at this lower temperature in pituitary cell membranes (Barros and Kaczorowski, 1984). Interestingly, even though the maximal initial transport rates are reduced about threefold at 25°C, the initial velocity of each process relative to the other remains the same. The maximal initial rate of Ca^{++} transport by Na^+-Ca^{++} exchange is two to three times greater than that of the Ca^{++}-pumping ATPase (Barros and Kaczorowski, 1984), which is consistent with our finding of a significant influence of Na^+-Ca^{++} exchange on the duration of the Ca^{++}-dependent Cl^- current.

Use of TEA^+ and TMA^+ to Inhibit Na^+-Ca^{++} Exchange

Several experiments indicate that under the conditions of these studies, substitution of TEA^+ for extracellular Na^+ prolonged Ca^{++}-dependent currents and facilitated rundown specifically by inhibiting Na^+-Ca^{++} exchange. The effects of TEA^+ on both Ca^{++} current rundown and Cl^- current duration, but not Ca^{++} current amplitude, were prevented by the addition of high intracellular [EGTA] (Fig. 4 *D*; see also Korn and Weight, 1987). This indicates that the effects of TEA^+ were dependent on intracellular Ca^{++} buffering. Ca^{++}-dependent Cl^- currents were prolonged even when bathing solutions were switched long after Ca^{++} channels had closed (Fig. 10), which demonstrates that the prolongation of Cl^- currents was not due to a direct effect of TEA^+ on Ca^{++} channels or Ca^{++} influx. Substitution of TMA^+ for Na^+ produced effects that were qualitatively identical to those of TEA^+ substitution, which indicates that the effects of TEA^+ substitution were not specific to TEA^+ or contaminants associated with it (Zucker, 1981). Ca^{++}-dependent Cl^- currents were prolonged by TEA^+ substitution in standard whole cell recordings with 80 mM HEPES in the pipette solution (Fig. 11), which indicates that the effects of Na^+ removal were not due to inhibition of Na^+-H^+ exchange. Finally, Ca^{++}-dependent Cl^- currents were not prolonged by Na^+ substitution when activated in the presence of fixed intracellular [Ca^{++}] (Fig. 12), which indicates that the prolongation observed in Figs. 8–10 was not due to a direct action of TEA^+ or Na^+ removal on Cl^- channels.

Other agents are available that block Na^+-Ca^{++} exchange, but none could be used in this study due to a lack of specificity. Substitution of Na^+ with Li^+ or NMG^+ reduced the voltage-activated Ca^{++} current and/or Ca^{++}-activated Cl^- current.

Replacement of Na^+ with Cs^+ resulted in a large inward leak current. The available drugs that block Na^+-Ca^{++} exchange, quinacrine and amiloride (Schellenberg et al., 1983; De La Pena and Reeves, 1987), blocked voltage-activated Ca^{++} currents at lower concentrations than are necessary to inhibit Na^+-Ca^{++} exchange (unpublished observations). Finally, we did not replace 150 mM Na^+ with choline because AtT-20s contain muscarinic cholinergic receptors (Heisler et al., 1983).

Function of Na^+-Ca^{++} Exchange

Since intracellular Ca^{++} plays a critical role in the secretion process, as well as so many other cellular processes, any mechanism that regulates intracellular Ca^{++} concentration will have functional significance. One obvious regulatory mechanism of Na^+-Ca^{++} exchange is simply the extrusion of intracellular free Ca^{++}, which may contribute to the turning off of Ca^{++}-dependent processes, and the clearing of intracellular Ca^{++} previously sequestered by intracellular buffers. The studies presented in this report indicate that Na^+-Ca^{++} exchange may also regulate intracellular Ca^{++} by another mechanism, namely, the regulation of Ca^{++}-dependent membrane currents, which play an important role in regulating the activity of voltage-gated Ca^{++} channels.

Use of the Perforated Patch Technique to Study the Endogenous Regulation of Intracellular Ca^{++} Transients

The perforated patch technique provides a useful tool for studying the functional consequences of cellular [Ca^{++}] regulation. As discussed above, endogenous Ca^{++} buffering processes cannot remain intact with the standard whole cell patch clamp technique. While the perforated patch technique is not a quantitatively accurate [Ca^{++}] detection method, it appears to be useful for monitoring qualitatively the time course of Ca^{++} transients near membrane-associated ion channels, without the cytoplasmic disruption associated with standard whole cell recording. At present, one limitation or another prevents any single Ca^{++} detection technique from providing a complete understanding of intracellular Ca^{++} regulation and its functional consequences. Ca^{++} indicator dyes, both absorbance and fluorescent, lack the spatial or temporal resolution to study the regulation of Ca^{++} transients very near the membrane surface on a time scale of milliseconds to hundreds of milliseconds. Ca^{++}-sensitive microelectrodes measure intracellular [Ca^{++}] at an undefined distance from the plasma membrane, and can be affected by changes in intracellular pH. Further, Ca^{++}-sensing techniques do not by themselves address the functional consequences of the observed cellular regulation of Ca^{++} transients. Pallotta et al. (1987) demonstrated that activation of single Ca^{++}-activated K^+ channels in cell-attached patches could be studied to accurately monitor [Ca^{++}] near the cytoplasmic surface of the plasma membrane. The perforated patch technique, while not providing the quantitative information about [Ca^{++}] that single K^+ channels provide, has the advantage of permitting the study of the functional consequences of altering endogenous Ca^{++} regulation on a variety of ion channel species. The combination of Ca^{++} dye and perforated patch techniques may provide important information towards this end.

We thank Shaiu Sun for maintenance of the cell lines, Archie Frunzy, and Eric Neugroschel for the design and construction of the magnetically driven stepping pipette holder, Drs. John Connor and John Reeves for interesting suggestions during the course of this work, and Drs. John Durkin and John Reeves for valuable comments on an earlier version of the manuscript. We also thank Dr. R. Fischmeister for bringing the possible involvement of Na^+-H^+ exchange to our attention.

Supported in part by National Institutes of Health Postdoctoral Fellowship NS-08117 to Dr. Korn.

Original version received 30 November 1988 and accepted version received 25 March 1989.

REFERENCES

Adler, M., B. S. Wong, S. Sabol, N. Busis, M. B. Jackson, and F. F. Weight. 1983. Action potentials and membrane ion channels in clonal anterior pituitary cells. *Proceedings of the National Academy Sciences.* 80:2086–2090.

Armstrong, C. M., and D. R. Matteson. 1985. Two distinct populations of calcium channels in a clonal line of pituitary cells. *Science.* 227:65–67.

Armstrong, D., and R. Eckert. 1987. Voltage-activated calcium channels that must be phosphorylated to respond to membrane depolarization. *Proceedings of the National Academy of Sciences.* 84:2518–2522.

Axelrod, J., and T. D. Reisine. 1984. Stress hormones: their interaction and regulation. *Science.* 224:875–877.

Barish, M. E., and S. H. Thompson. 1983. Calcium buffering and slow recovery kinetics of calcium-dependent outward current in molluscan neurons. *Journal of Physiology.* 337:201–219.

Barrett, J. N., K. L. Magleby, and B. S. Pallotta. 1982. Properties of single calcium-activated potassium channels in cultured rat muscle. *Journal of Physiology.* 331:211–230.

Barros, F., and G. J. Kaczorowski. 1984. Mechanisms of Ca^{2+} transport in plasma membrane vesicles prepared from cultured pituitary cells. II. (Ca^{2+} + Mg^{2+})-ATPase-dependent Ca^{2+} transport activity. *Journal of Biological Chemistry.* 259:9404–9410.

Bean, B. P. 1985. Two kinds of calcium channels in canine atrial cells. *Journal of General Physiology.* 86:1–30.

Belles, B., J. O. Karlsson, J. Hescheler, and W. Trautwein. 1988*a*. Effect of the Ca^{2+}-dependent protease calpain and its inhibitor calpastatin on the "run-down" of cardiac Ca^{2+} current. *Pflügers Archiv.* 411:R21. (Abstr.)

Belles, B., C. O. Malecot, J. Hescheler, and W. Trautwein. 1988*b*. "Run-down" of the Ca current during long whole cell recordings in guinea pig heart cells: role of phosphorylation and intracellular calcium. *Pflügers Archiv.* 411:353–360.

Blaustein, M. P., R. W. Ratzlaff, N. C. Kendrick, and W. S. Schweitzer. 1978. Calcium buffering in presynaptic nerve terminals. I. Evidence for involvement of a nonmitochondrial ATP-dependent sequestration mechanism. *Journal of General Physiology.* 72:15–41.

Byerly, L., and S. Hagiwara. 1982. Calcium currents in internally perfused nerve cell bodies of *Limnea stagnalis. Journal of Physiology.* 322:503–528.

Byerly, L., and B. Yazejian. 1986. Intracellular factors for the maintenance of calcium currents in perfused neurons from the snail, *Lymneea stagnalis. Journal of Physiology.* 370:631–650.

Cass, A., A. Finkelstein, and V. Krespi, 1970. The ion permeability induced in thin lipid membranes by the polyene antibiotics nystatin and amphotericin B. *Journal of General Physiology.* 56:100–124.

Chad, J. E., and R. Eckert. 1986. An enzymatic mechanism for calcium current inactivation in dialysed *Helix* neurones. *Journal of Physiology.* 378:31–51.

Chapman, R. A. 1986. Sodium/calcium exchange and intracellular calcium buffering in ferret myocardium: an ion sensitive microelectrode study. *Journal of Physiology.* 373:163–179.

Connor, J. A., and G. Nikolakopoulou. 1982. Calcium diffusion and buffering in nerve cytoplasm. *Lectures on Mathematics in the Life Sciences.* 15:79–101.

De La Pena, P., and J. P. Reeves. 1987. Inhibition and activation of Na^+-Ca^{2+} exchange activity by quinacrine. *American Journal of Physiology.* 252:C24–C29.

DeRiemer, S. A., and B. Sakmann. 1986. Two calcium currents in normal rat anterior pituitary cells identified by a plaque assay. *Experimental Brain Research.* 14:139–154.

Doroshenko, P. A., P. G. Kostyuk, A. E. Martynuk, and M. D. Kursky. 1982. Intracellular metabolism of adenosine 3'-5'-cyclic monophosphate and calcium inward current in perfused neurones of *Helix pomatia. Neuroscience.* 7:2134–2155.

Doroshenko, P. A., P. G. Kostyuk, A. E. Martynuk, M. D. Kursky, and Z. D. Verobetz. 1984. Intracellular protein kinase and calcium inward currents in perfused neurones of the snail *Helix pomatia. Neuroscience.* 11:263–267.

Dubinsky, J. M., and G. S. Oxford. 1984. Ionic currents in two strains of rat anterior pituitary tumor cells. *Journal of General Physiology.* 83:309–339.

Eckert, R., J. E. Chad, and D. Kalman. 1986. Enzymatic regulation of calcium current in dialyzed and intact molluscan neurons. *Journal de Physiologie.* 81:318–324.

Evans, M. G., and A. Marty. 1986. Calcium-dependent chloride currents in isolated cells from rat lacrimal glands. *Journal of Physiology.* 378:437–460.

Fenwick, E. M., A. Marty, and E. Neher. 1982. Sodium and calcium channels in bovine chromaffin cells. *Journal of Physiology.* 331:599–635.

Forscher, P., and G. S. Oxford. 1985. Modulation of calcium channels by norepinephrine in internally dialyzed avian sensory neurons. *Journal of General Physiology.* 85:743–763.

Gill, D. L., S.-H. Chueh, and C. L. Whitlow. 1984. Functional importance of the synaptic plasma membrane calcium pump and sodium-calcium exchanger. *Journal of Biological Chemistry.* 259:10807–10813.

Hamill, O. P., A. Marty, E. Neher, B. Sakmann, and F. J. Sigworth. 1981. Improved patch-clamp techniques for high-resolution current recording from cells and cell-free membrane patches. *Pflügers Archiv.* 381:85–100.

Heisler, S., L. Larose, and J. Morisset. 1983. Muscarinic cholinergic inhibition of cyclic AMP formation and adrenocorticotropin secretion in mouse pituitary tumor cells. *Biochemistry and Biophysics Research Communications.* 114:289–295.

Henkart, M. P., T. S. Reese, and F. J. Brinley, Jr. 1978. Endoplasmic reticulum sequesters calcium in the squid giant axon. *Science.* 202:1300–1303.

Hess, P., A. P. Fox, J. B. Lansman, B. Nilius, M. C. Nowycky, and R. W. Tsien. 1986. Calcium channel types in cardiac, neuronal and smooth muscle-derived cells: differences in gating, permeation and pharmacology. *In* Ion Channels in Neural Membranes. J. M. Richie, R. D. Keynes, L. Bolis, editors. Alan R. Liss Inc., New York. 227–252.

Holz, R., and A. Finkelstein. 1970. The water and nonelectrolyte permeability induced in thin lipid membranes by the polyene antibiotics nystatin and amphotericin B. *Journal of General Physiology.* 56:125–145.

Horn, R., and A. Marty. 1988. Muscarinic activation of ionic currents measured by a new whole cell recording method. *Journal of General Physiology.* 92:145–159.

Horn, R., A. Marty, and S. J. Korn. 1988. Perforated patch recording to prevent wash-out. *Biophysical Journal.* 53:360*a*. (Abstr.)

Kaczorowski, G. J., L. Costello, J. Dethmers, M. J. Trumble, and R. L. Vandlen. 1984. Mechanisms of Ca^{2+} transport in plasma membrane vesicles prepared from cultured pituitary cells. I. Characterization of Na^+/Ca^{2+} exchange activity. *Journal of Biological Chemistry.* 259:9395–9403.

Kidokoro, Y. 1975. Spontaneous calcium action potentials in a clonal pituitary cell line and their relationship to prolactin secretion. *Nature.* 258:741–742.

Kolesnick, R. N., and M. C. Gershengorn. 1986. Thyrotropin-releasing hormone stimulation of prolactin secretion is coordinately but not synergistically regulated by an elevation of cytoplasmic calcium and 1,2-diacylglycerol. *Endocrinology.* 119:2461–2466.

Korn, S. J., and R. Horn. 1989. Influence of sodium-calcium exchange on pituitary cell membrane currents. *Biophysical Journal.* 55:172*a*. (Abstr.)

Korn, S. J., and F. F. Weight. 1987. Patch-clamp study of the calcium-dependent chloride current in AtT-20 pituitary cells. *Journal of Neurophysiology.* 57:325–340.

Luini, A., D. Lewis, S. Guild, D. Corda, and J. Axelrod. 1985. Hormone secretagogues increase cytosolic calcium by increasing cAMP in corticotropin-secreting cells. *Proceedings of the National Academy of Sciences.* 82:8034–8038.

Luini, A., D. Lewis, S. Guild, G. Scholfield, and F. F. Weight. 1986. Somatostatin, an inhibitor of ACTH secretion, decreases cytosolic free calcium and voltage-dependent calcium current in a pituitary cell line. *Journal of Neuroscience.* 6:3128–3132.

Marty, A., and A. Finkelstein. 1975. Pores formed in lipid bilayer membranes by nystatin. *Journal of General Physiology.* 65:515–526.

Mollard, P., P. Vacher, J. Guerin, M. Rogowski, and B. Dufy. 1987. Electrical properties of cultured human ACTH-secreting adenoma cells: effects of high K, cortocotropin-releasing factor and angiotensin II. *Endocrinology.* 121:395–405.

Pallotta, B. S., J. R. Hepler, S. A. Oglesby, and T. K. Harden. 1987. A comparison of calcium-activated potassium channel currents in cell-attached and excised patches. *Journal of General Physiology.* 89:985–997.

Ritchie, A. K. 1987. Two distinct calcium-activated potassium currents in rat anterior pituitary cell line. *Journal of Physiology.* 385:591–609.

Schellenberg, G. D., L. Anderson, and P. D. Swanson. 1983. Inhibition of Na^+-Ca^{2+} exchange in rat brain by amiloride. *Molecular Pharmacology.* 24:251–258.

Schlegel, W., B. P. Winiger, P. Mollard, P. Vacher, F. Wuarin, G. R. Zahnd, C. B. Wollheim, and B. Dufy. 1987. Oscillations of cytosolic Ca^{2+} in pituitary cells due to action potentials. *Nature.* 329:719–721.

Suprenant, A. 1982. Correlation between electrical activity and ACTH/β-endorphin secretion in mouse pituitary tumor cells. *Journal of Cell Biology.* 95:559–566.

Taraskevich, P. S., and W. W. Douglass. 1977. Action potentials occur in cells of the normal anterior pituitary gland and are stimulated by the hypophysiotropic peptide thyrotropin-releasing hormone. *Proceedings of the National Academy of Sciences.* 74:4064–4067.

Wong, B. S., H. Lecar, and M. Adler. 1982. Single calcium-dependent potassium channels in clonal anterior pituitary cells. *Biophysical Journal.* 39:313–317.

Zatz, M., and T. D. Reisine. 1985. Lithium induces corticotropin secretion and desensitization in cultured anterior pituitary cells. *Proceedings of the National Academy of Sciences.* 82:286–1290.

Zucker, R. S. 1981. Tetraethylammonium contains an impurity which alkalizes cytoplasm and reduce calcium buffering in neurons. *Brain Research.* 208:473–478.